



RESEARCH ARTICLE

Extraction of synephrine from waste peels of *Citrus sinensis* and green synthesis of gold nanoparticles from it against Dermatophytes

Ayat Subhi Jadou & Rusol AL-Bahrani

Department of Biology, Collage of Science, University of Baghdad, Baghdad, Iraq

*Email: rusol.jasim@sc.uobaghdad.edu.iq



ARTICLE HISTORY

Received: 03 January 2024

Accepted: 08 March 2024

Available online

Version 1.0 : 31 March 2024



Additional information

Peer review: Publisher thanks Sectional Editor and the other anonymous reviewers for their contribution to the peer review of this work.

Reprints & permissions information is available at https://horizonepublishing.com/journals/index.php/PST/open_access_policy

Publisher's Note: Horizon e-Publishing Group remains neutral with regard to jurisdictional claims in published maps and institutional affiliations.

Indexing: Plant Science Today, published by Horizon e-Publishing Group, is covered by Scopus, Web of Science, BIOSIS Previews, Clarivate Analytics, NAAS, UGC Care, etc See https://horizonepublishing.com/journals/index.php/PST/indexing_abstracting

Copyright: © The Author(s). This is an open-access article distributed under the terms of the Creative Commons Attribution License, which permits unrestricted use, distribution and reproduction in any medium, provided the original author and source are credited (<https://creativecommons.org/licenses/by/4.0/>)

CITE THIS ARTICLE

Jadou AS, Bahrani RA. Extraction of synephrine from waste peels of *Citrus sinensis* and green synthesis of gold nanoparticles from it against Dermatophytes. Plant Science Today (Early Access). <https://doi.org/10.14719/pst.3248>

Abstract

The main object of the current work was to determine the antifungal efficiency of secondary metabolites product called synephrine that extracted from *Citrus sinensis* peels and the ability of synephrine to biosynthesis gold nanoparticles from HAuCl₄ which consider environmentally favourable method, then determine their activity against pathogenic human dermatophyte. The identification of synephrine done by Thin layer chromatography (TLC), High Performance Liquid Chromatography (HPLC) and The Fourier Transform Infrared (FTIR). The characterization of gold nanoparticles by using Ultra Violet-Visible Spectroscopy (UV-Vis), Field – Emission Scanning Electron Microscopy (FESEM) and Fourier Transform Infrared (FTIR), confirmed the biosynthesis of gold nanoparticles in diameter and morphology for AuNps biosynthesis by *C. sinensis* was 9.7-31 (nm) rounded to oval shape. The synephrine and AuNps that formed use it against some dermatophytes *Trichophyton mentographytes*, *Trichophyton rubrum* and *Microsporum canis*, the activity of synephrine against *T. mentographytes* at (10, 15 and 20 mg/mL) give less inhibition effect as compare with antifungal effect, while *M. canis* in 15 mg/mL show best effect than antifungal and for gold nanoparticles most concentration effective was (20 mg/mL).

Keywords

AuNps; *Citrus sinensis* ; dermatophyte; synephrine

Introduction

One of the most popular and significant citrus species is *Citrus sinensis*. It's important to note that sweet orange peel secondary metabolites have demonstrated antibacterial and antifungal effects, making *C. sinensis* peel a very significant fruit waste. The amount of alkaloid compounds in the CS was linked to its antioxidant activity, which was demonstrated by numerous researches. Along with that, due to its capacity to scavenge free radicals, protoalkaloid are most likely the most significant natural alkaloid in CS, the *C. sinensis* peels have shown to have antibacterial and antifungal effects. A study explored the effects of peels extracts from *C. sinensis* as antifungal inhibition and formation of gold nanoparticles (4). Synephrine (C₉H₁₃NO₂) is a kind of alkaloid obviously existing in *C. sinensis* (5). Chemically and structurally, p-synephrine, octopamine (nor-synephrine) and m-synephrine (phenylephrine) are like ephedrine. Synephrine is classified as an unspecific adrenergic agonist, with the ability to occur in 3 distinct positional isomers,

namely ortho (o-), para (p-) and meta (m-) (6). Dermatophytes are a group of molds able to produce keratinase (1). According to reports, 1.7 million mortalities from fungal infections are expected in 2020. Given the rising increase in fungus infections, medical professionals face a great challenge when selecting antifungal treatments. This rise related to the growth in immunocompromised individuals brought on by modifications in therapeutic practice, such as the use of potent immunosuppressive drugs and intensive chemotherapy (2). *Trichophyton rubrum*, *T. mentagrophytes* and *M. canis* are the main dermatophyte species found in Europe, the Eastern Mediterranean region and South America. Because dermatophytes thrive in warm, humid climates, they are more prevalent in tropical. Dermatophytes exhibit an important tendency to infect individuals across all demographics, including individuals of all ages, races, genders and socioeconomic backgrounds. Furthermore, these fungal pathogens are capable of infecting both domestic and wild animals, whatever their health states or epidemiological situations, according to evidence from countless observational studies carried out over the past 90 years (3). The study of nanotechnology has received a lot of attention recently. It deals with nanoparticles, which are widely employed in atomic physics, medical chemistry, and all other domains that are currently known. Nanoparticles range in size from 1 to 100 nm in one dimension. The primary reasons why nanoparticles are used are their small size, oriented shape and physical characteristics, which have been found to alter the interaction between other materials they encounter. It is simple to create these particles using various chemical, physical and biological methods. The fastest emerging method of preparation is the biological approach (7). It is important to be an efficient antimicrobial agent with little human toxicity and a variety of *in vitro* and *in vivo* uses (8). The AuNP biological technique, which uses microbes, enzymes and physical methods. Plant mediated nanoparticle synthesis is favoured among the available synthesis techniques because it is economical, environmentally benign and suitable for human medicinal usage (9). Plant extracts, has recently been proposed as having many advantages over both chemical and physical.

Green Synthesis of Nanoparticles

Due to the use of affordable and non-hazardous raw materials, green synthesis is seen as a potential technique for the synthesis of NPs. One of the finest options for producing AuNPs on a wide scale with clearly specified size and morphology is this low-cost, plant-based green synthesis process (10). The sustained production of NPs in plants has excellent therapeutic efficacy, low toxicity, and is focused binding and delivery that is site-specific. Additionally, this has little impact on human health because fungus and bacteria are favored candidates for NP production over microorganisms in the environment (11). Nonetheless, the synthesis of NPs often involves plants and does not need the difficult process of maintaining microbial cultures. Because of applications for and methods of characterization in cancer therapy and diagnosis. The utilization of plant-based green synthesis

methods is a highly viable approach towards minimizing the economic burden associated with anticancer interventions. The process of synthesizing gold nanoparticles (AuNPs) on a massive scale, while ensuring their size and morphology are well-defined as well as their probable mechanisms of action on.

Materials and Methods

Collection of Plant Samples

This study included the use the peels *C. sinesnsis* and was collected from markets, Iraq. The plants were identified at the herbarium. The plant material was subjected to mechanical grinding, resulting in dry and powdered form. The resulting powder was then stored at a temperature of 4 °C for subsequent analysis.

Extraction of Synephrine from Peels

100 g of dried powdered fruit peels of Iraqi *C. sinesnsis* was defatted with n-hexane for 24 h and permitted to undergo the drying process at the ambient temperature of the room. The soxhlet extractor filled with the defatted plant material, which was held in a thimble. In a 1 L round bottom flask equipped with a Soxhlet extractor, 500 mL of 80% methanol was utilized as the solvent. For another 12 h, the extraction was continued. 2N hydrochloric acid add to extract in order to dissolve it then shook it on a water bath, filtered and concentrated under decreased pressure to dryness using operating a rotating evaporator at a temperature lower than 40°C.

The resultant filtrate was then shaken with chloroform to eliminate undesirable components. Alkaloid bases were liberated from the acidic aqueous layer by correcting the pH with ammonia to an alkaline level and then the aqueous layer was concentrated under vacuum (12).

Identification of Synephrine By TLC

The isolation of synephrine achieved through the application of preparative layer chromatography. This method involved the use of glass plates measuring 20 cm × 20 cm, which were coated with a 2 mm thick layer of silica gel GF 254. The coating process was carried out using a laboratory division TLC coater. The peel extract was administered by applying it in a linear arrangement of dots utilizing a capillary tube. The reference standard of synephrine was positioned to the right of the baseline. The extract was applied 4 times in each plate, with a waiting period following each application until complete solvent evaporation (14). The detection process involved the utilization of a spraying reagent composed of 2% ninhydrin in n-butanol. A specific section of the plate, located on the right side and corresponding to the synephrine standard, was designated for spraying with the 2% ninhydrin reagent. In contrast, the remaining portion of the plate was shielded from spraying by a glass plate. The bands associated with the synephrine standard were carefully removed and accumulated in a container. Subsequently, they were subjected to elution using mild heating and filtration. The resulting filtrate was then evaporated under reduced pressure until complete dryness, resulting in the formation of a white precipitate (15).

Qualitative of Synephrine By HPLC

Synephrine was estimated both qualitatively and quantitatively using HPLC. Using (Knauer/Germany), HPLC analysis was performed. By comparing the retention durations obtained from examined materials with genuine standards under identical chromatographic conditions, identifications were made. The column utilized was C18 (150 mm 4.6 mm/5 μ m), the mobile phase was acetonitrile: water: orthophosphoric acid 0.1% acid (30:70) and the rate of flow was 0.6 mL/min with UV detection, 220 nm detector (16).

Gold Salt

The chloroauric acid (HAuCl₄) used in this study was bought from Sigma Aldrich, the remaining reagents employed in the process were of analytical grade, ensuring the highest level of purity. The experiment utilized deionized water as the primary solvent.

Biosynthesis Method of Gold Nanoparticles

Plant peels are used in the biosynthesis process to create gold nanoparticles. The peels are cleaned in (D.W) distilled water, chopped into little pieces and then boiled in the universal solvent (D.W) to produce extract. By employing various techniques including filtering and centrifugation, the extract can be further refined (17). Simply combining the extract with the auric salts solution at room temperature causes them to transform into nanoparticles in a quick, easy and environmentally friendly process. Phytochemicals serve as both stabilizing and reducing agents, hence no further external stabilizing or capping agents are required. To reduce the metal salt, the reaction mixture is further incubated and the color change is used for visual monitoring (18).

Characterization of the Prepared Nanoparticles

Ultraviolet-Visible Spectroscopy

The term "ultraviolet-visible spectrophotometer (UV Vis)" is used to describe a technique known as absorption spectroscopy. The samples were subjected to measurement using (UV-Vis) double beam spectrophotometers within the wavelength range of 400-800 nm.

Characterization of AuNPs Using Field – Emission Scanning Electron Microscopy (FESEM)

Utilise electrons as an alternative to light sources for the purpose of examining the topographical characteristics of objects. The electrons generated by the field emission source undergo acceleration in the direction of a pronounced gradient in the electrical field. The concentration of primary electrons occurs within a high vacuum column, wherein an electronic lens is utilised to deflect the emitted electrons towards individual objects. Every individual object releases secondary emission electrons in this manner. The surface properties of an object exert a significant influence on the velocity and angle of secondary electrons. The electrons are captured by a detector, which subsequently generates an electrical signal. A video scan is conducted on the aforementioned signal. The signal undergoes a change that leads to the production of a video-scan image. The aforementioned image can be visually examined on a display screen and subsequently kept for

future analysis. The provided text lacks sufficient information to be rewritten in an academic manner (19).

Fourier Transform Infrared (FTIR)

The functional groups present on AuNPs were verified through the utilization of Fourier-transform infrared (FTIR) spectroscopy within the spectral region of 400-4000 cm^{-1} (20).

Antifungal Assay Activity

The investigation involved assessing the antifungal activity of synephrine and AuNPs, which were produced from an extract, in a dose-dependent way using the well diffusion method. The fungal isolates were cultivated in a broth medium known as potato dextrose broth (PDB) for a duration of 7 to 10 days, and these cultures were subsequently utilized for the purposes of the investigation. The microorganism was generated by evenly distributing 100 mL of a revived culture, which contained 10⁴ cells mL⁻¹, onto (PDA) potato dextrose agar media from Hi Media, using a spreader (21). Different concentrations of extract and Au NPs (10, 15 and 20 mg/mL) were introduced into the central region of a well with a diameter of 7 mm.

The positive and negative controls for the antifungal assay consisted of candidstain and distilled water respectively. The petri plates were incubated at a temperature of 25 °C for a duration of 7-10 days in an incubator. During this incubation period, the presence of growing colonies (measured in mm) surrounding the well indicated the activity (22).

Results

TLC Detection

A lonely circular and condensed area, exhibiting same color and closely value for R_f as calculated R_f value for synephrine *C. sinensis* 0.28 and 0.25 as the reference standard, was observed on thin-layer chromatography (TLC) plates when subjected to 5 distinct developing solvent systems as show in Fig. 1. This finding serves as confirmation of the existence of synephrine within the extract derived from the peels of Iraqi *C. sinensis* fruits.

HPLC Detection

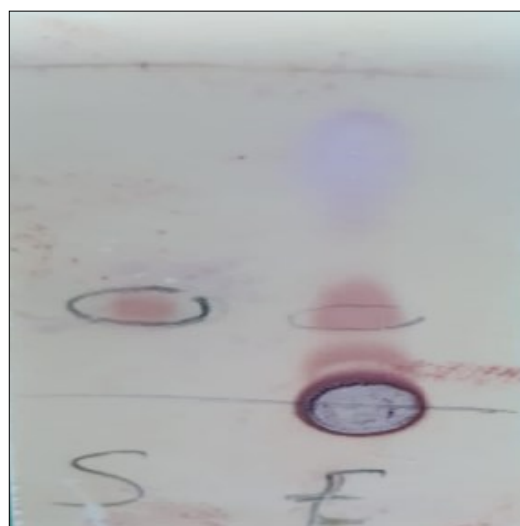


Fig. 1. Synephrine from *C. sinensis* and stander.

HPLC was used to further confirm the presence of synephrine in Iraqi *C. sinensis* fruit peels. A peak was found in the chromatogram of the extract of Iraqi *C. sinensis* fruit peels that had the same retention time (6.3 min) as the synephrine reference standard, indicating that the peak was most likely synephrine as seen in Fig. 2 and 3.

FESEM micrograph revealed the particle size range to be (9-31) nm. The coexistence of Au NPs in lower and bigger sizes was caused by those created During the initial and afterwards stages of the process, demonstrating that nucleation to form new NPs and aggregation to form larger particles occurred concurrently. The spot profile EDX of Au NPs, as seen in Fig. 5, revealed significant signals for gold atoms alongside weak signals from carbon and oxygen.

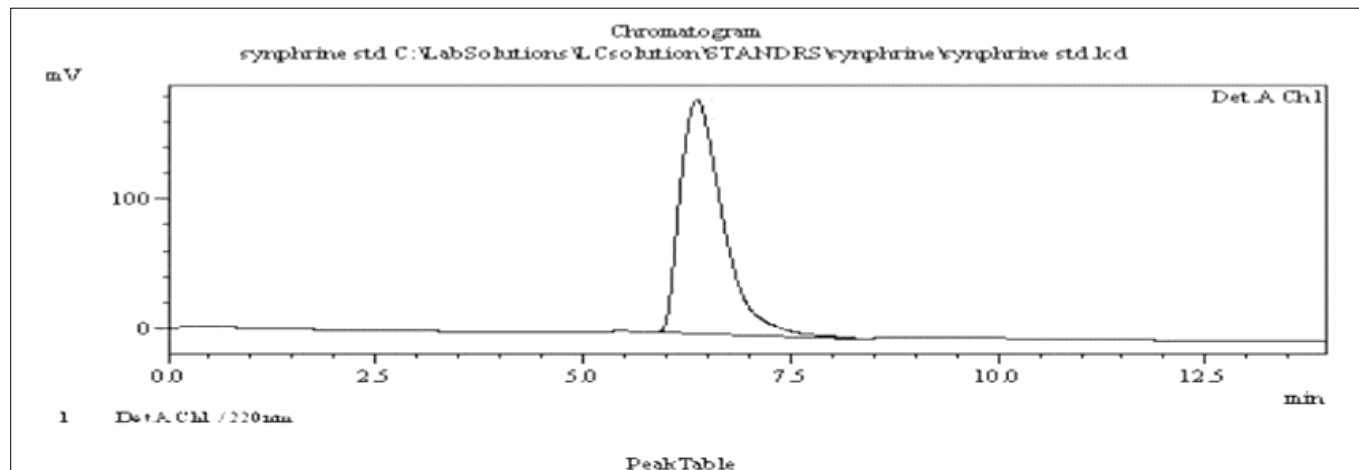


Fig. 2. HPLC of synephrine stander.

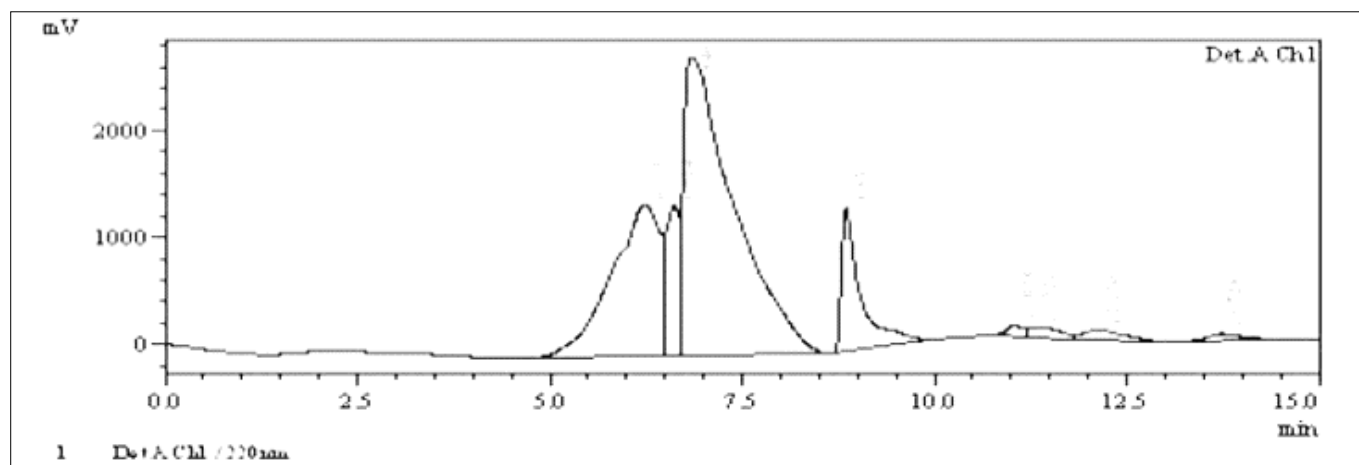


Fig. 3. HPLC of synephrine in the extracted *Citrus sinensis* peels.

UV Spectrophotometry Study

The results of the UV-visible absorption spectra show a novel method for making the Au NPs. There was a rise in intensity up to 10 min as a function of time without any change in the peak wavelength and the scale of wavelength was stable between 400 and 800 nm. The surface plasmon resonance (SPR) of the Au NPs generated resembled to 470 nm as show in Fig. 4.

FESEM Study

Using FESEM, the morphology of NPs surface was studied. The microscopy examination revealed that even within the aggregates, produced Au NPs were not in direct contact, indicating that the NPs had stabilized. The majority of the biosynthesized Au NPs were discovered to have spherical forms; the forms of morphology and dimensions of the aggregations were described (23). The study shows that the reducing process is maintained in the surface. After 10 min of reaction time at pH 7.0, the Au NPs' histogram of particle size distribution was obtained. A representative

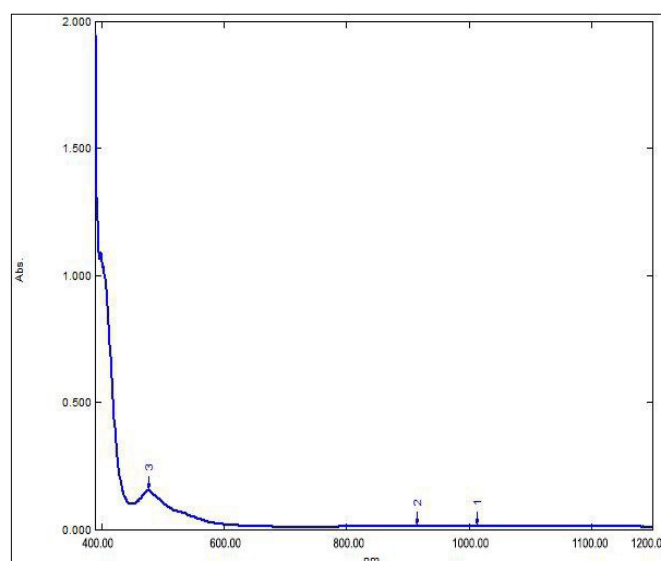


Fig. 4. UV-visible spectrum of synthesized Au NPs showed peak at 470 nm.

These flimsy signals may have resulted from macromolecules like proteins or enzymes that were either bound to the NPs or nearby and emit X-rays.

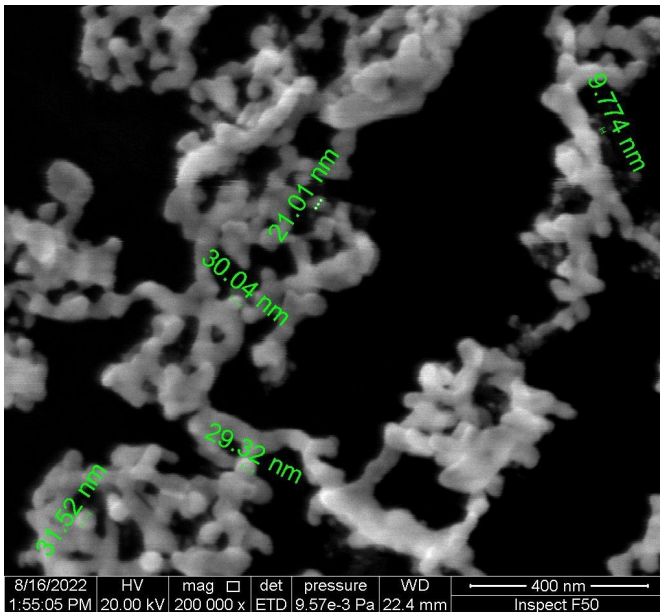


Fig. 5. FESM images of the synthesized Au NPs the spherical morphology appearance and diameter.

Fourier-Transform Infrared Spectroscopy (FTIR)

The Fourier transform infrared (FTIR) approach is a spectroscopic practice that enables identification of changes in the overall composition of biomolecules by detecting alterations in functional groups. Fourier Transform Infrared Spectroscopy (FTIR) is a widely employed analytical technique that enables the measurement of molecular vibrations and rotations induced by infrared radiation. By detecting structural differences in the binding of molecules, one can gather information regarding the presence of their interactions. The primary methods employed in the characterization of materials using Fourier Trans-

form Infrared (FTIR) spectroscopy include transmittance FTIR, attenuated total reflectance (ATR-FTIR) and micro-spectroscopy FTIR (24).

Fig. 6 showed the presence of aliphatic peak at (2813 cm^{-1}), while the hydroxyl groups appeared in the form of a broad peak at ($3170\text{--}3394\text{ cm}^{-1}$), while the secondary amine group appeared in the form of a single peak at (3029 cm^{-1}). The most important group in this compound is the presence of meta compensation on the ring, and this constitutes a peak that is considered a fingerprint of the compound between $1667\text{--}2000\text{ cm}^{-1}$.

Fig. 7 showed the presence of aliphatic aggregates at (2812 cm^{-1}), while the hydroxyl groups appeared in the form of a broad peak at ($3170\text{--}3384\text{ cm}^{-1}$), while the secondary amine group appeared in the form of a single peak at (3049 cm^{-1}). The most important group in this compound is the presence of meta compensation on the ring, and this constitutes a peak that is considered a fingerprint of the compound between ($1631\text{--}1764\text{ cm}^{-1}$) the presence of gold appearance near the peak 890 cm^{-1} .

Antifungal Activity of Synephrine Extracted from Peels of *C. sinensis*

The effect of synephrine extracted from peels of *C. sinensis* against the 3 types of fungal as shown in Table 1 the statistics show that *T. mentographytes* at (10, 15 and 20 mg/mL) give less inhibition effect as compare with antifungal effect ,while *Microsporium canis* in 15 mg/mL show best effect than antifungal that's give as an idea to suggest to prepare ointment against *T. mentographytes* and *M. canis* in 15 mg/mL .There is no significant effect for other con-

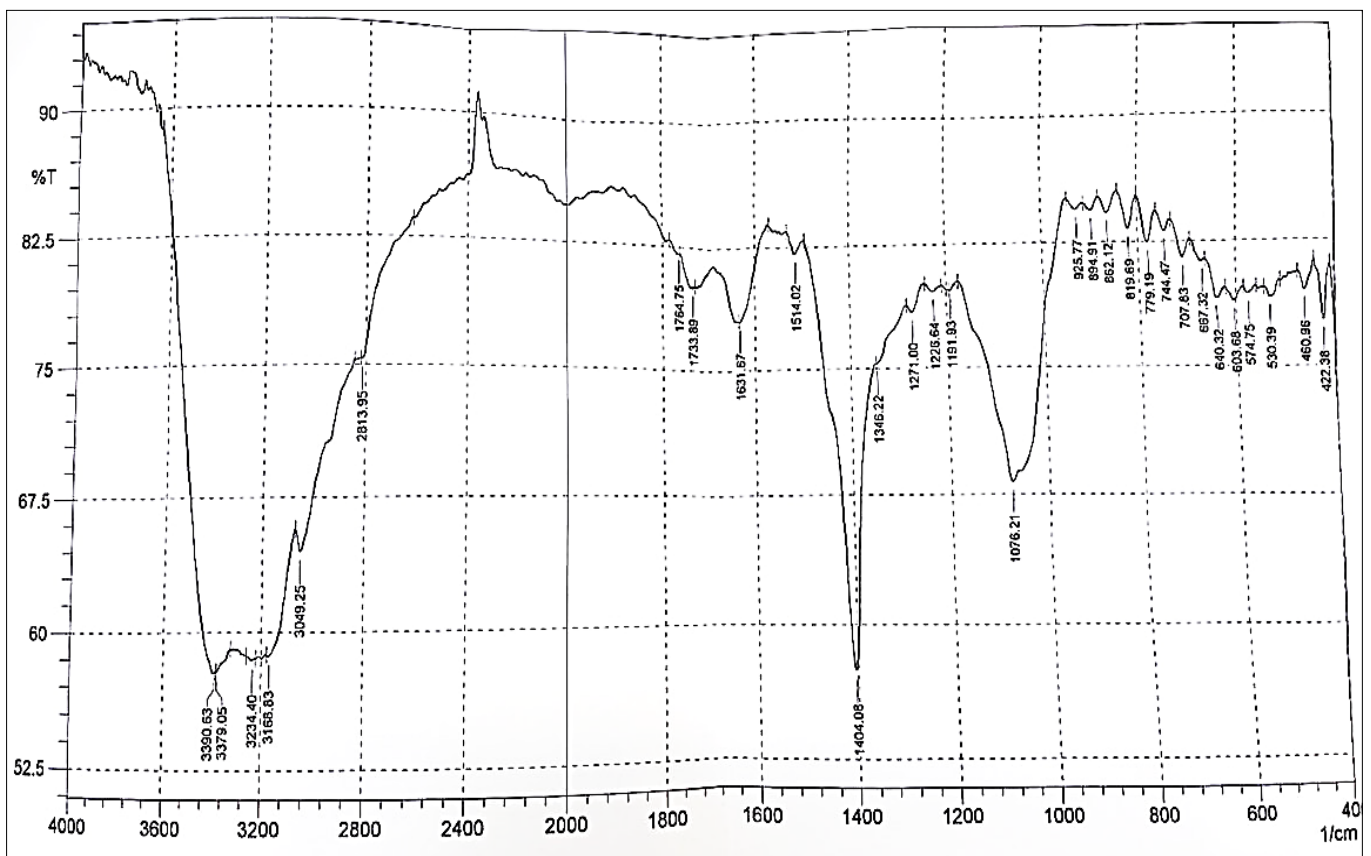


Fig. 6. FTIR analysis for *C. sinensis*.

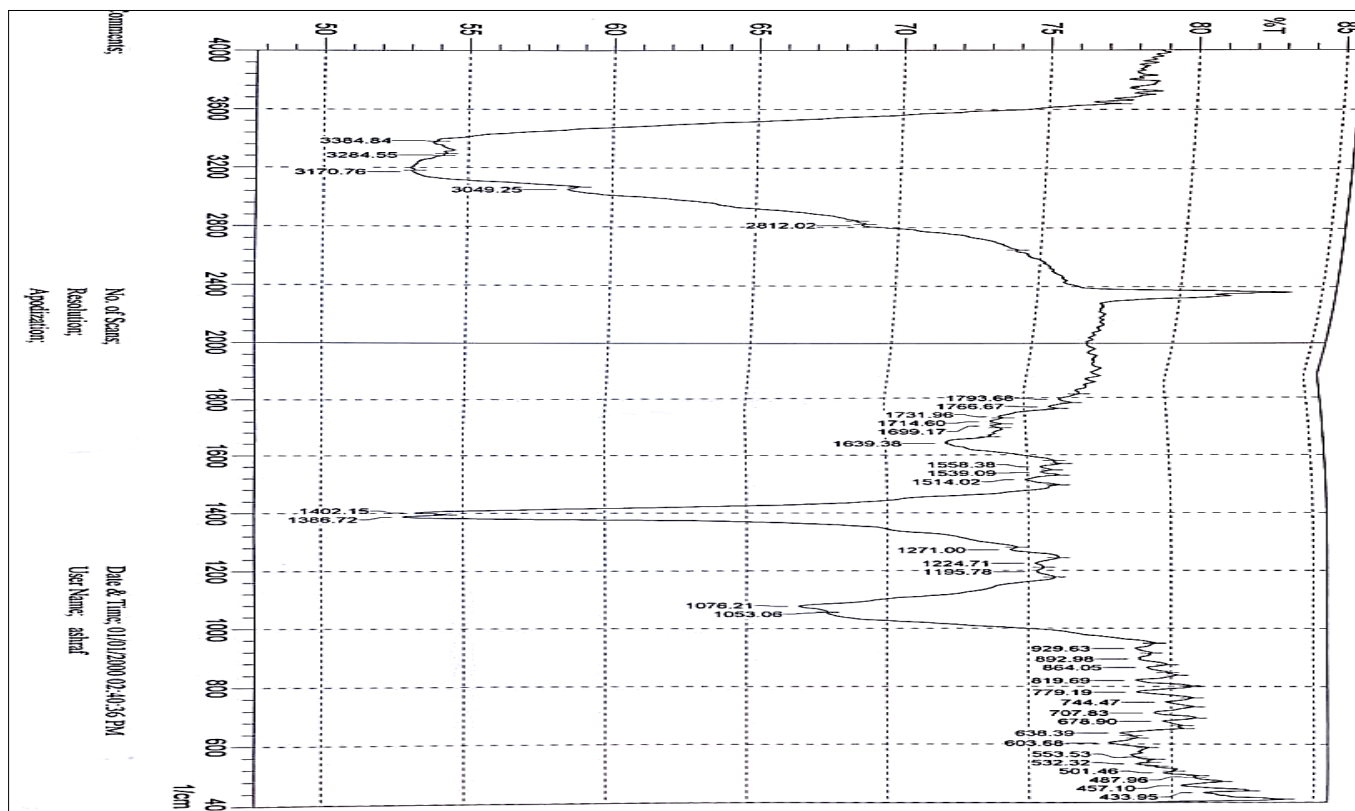


Fig. 7. FTIR analysis for *C. sinensis*.

Table 1. MIC Of *C. sinensis* against dermatophytes.

Diameters of fungi	Concentration of <i>C. sinensis</i>			Antifungal candstatin	Control	Mean
	10 mg/mL	15 mg/mL	20 mg/mL			
Trichophyton mentogrophytes	3.750	3.917	3.167	2.083	6.667	3.917
<i>Trichophyton rubrum</i>	2.750	1.833	3.167	2.000	6.800	3.310
<i>Microsporum canis</i>	2.333	1.417	2.017	2.000	6.000	2.753
lsd5%			NS			0.489**
Mean	2.944	2.389	2.784	2.028	6.489	
lsd5%			0.631**			

centration, genus and antifungal which used in experiment but despite of the little differences effect. The range of side effects associated with antifungal medications exhibits variability. The outcomes are dependent upon the specific medicine, dosage and fungal species. The individual suffers from symptoms of abdominal pain, gastrointestinal discomfort and loose bowel movements. The individual may have a sense of burning or the development of a rash on the skin. Infrequently, the administration of an antifungal medication may give rise to significant complications, such as hepatotoxicity leading to the manifestation of jaundice. Severe allergic reactions, such as anaphylaxis, can occur in certain individuals. Severe cutaneous hypersensitivity reactions, characterized by the formation of blisters and exfoliation of the epidermis (25).

Antifungal Activity of Gold Nanoparticles

AS in Table the effect of gold nanoparticles and the control on the inhibition of molds growth used in this study was observed. When the gold nanoparticles were applied to the samples, the diameter of the mold colonies was less than the diameter of the colonies over which

control was applied and the diameter was larger than that of control. Table 2 showed the most concentration effective for was (15 mg/mL) because the growth was inhibited more than the other 2 concentration (10, 20 mg/mL) in *T. mentogrophytes*. It the previous table showed had inhibition effect on growth when treat with gold nanoparticles (15 mg/mL), on *M. canis* which was more affected than other species. It followed by, *T. rubrum* in it inhibited when treated by gold nanoparticles that mean the gold nanoparticles had the strong effect on this species by make less capability of growth for these cells of species. Each other had inhibited effect when treat by gold nanoparticles, this material can be used as therapy for these isolated pathogenic fungi, *T. rubrum* and *T. mentogrophytes*. The results of their response to gold nanoparticles were very close to each other, that means the gold nanoparticles effected on the growth of this species, comparable to the control, the control had no effect on this species. This result, demonstrated this species had inhibitory response when treated by gold nanoparticles (26).

Table 2. MIC of gold nanoparticles biosynthesis from *C. sinensis* against dermatophyte.

Diameters of fungi	Concentration of <i>C. sinensis</i>			Antifungal candstatin	Control	Mean
	10 mg/mL	15 mg/mL	20 mg/mL			
Trichophyton mentographytes	4.080	3.670	5.170	2.070	4.900	3.978
<i>Trichophyton rubrum</i>	2.050	3.670	1.830	2.000	5.330	2.976
<i>Microsporum canis</i>	2.000	1.330	2.170	2.000	5.500	2.600
I _{sd} 5%			1.203**			0.538**
Mean	2.710	2.890	3.057	2.023	5.243	
I _{sd} 5%			0.694**			

Discussion

Plants produce various type and amount of secondary metabolic compounds including alkaloids, phenols, tanins etc. The widest spectrum of pharmacological action is exhibited by alkaloids synephrine is type of protoalkaloid which have antimicrobial effect (27). Isolation and identification of synephrine was done by TLC and HPLC. Extraction from *C. sinensis* peels have important roles in recycling waste.

The Au NPs generated using green methods exhibit a lack of unwanted or harmful contaminations. Therefore, it is plausible that this green-synthesized nanoparticle possesses efficacy in eradicating various pathogens, including bacteria, fungus and yeasts (28). The synthesis of AUNPs is confirmed by various characterisation techniques, including FESEM, EDS, FTIR and (UV)-Vis spectrophotometry (29).

When gold come into contact with the cellular membrane of microbial cells, it is possible for the generation of Reactive Oxygen Species (ROS) to occur. Reactive Oxygen Species (ROS) have been observed to decrease bacterial adhesion and induce fungi cell death by disrupting the integrity of the cell wall, interfering with the modification of cytosolic enzymes involved in respiration to macromolecular structures, affecting cellular integrity and gene expression, as well as inhibiting phosphate absorption and cellular communication (30).

Several theories have been suggested about the antimicrobial of nanoparticle solutions. Several possible processes have been suggested, one of which involves altering the permeability of the cell membrane. This modification allows for the interaction with DNA, proteins and other cell constituents containing phosphorus and sulfur, which are detrimental to fungi. Another method involves the generation of free radicals, which are responsible for causing damage to the membrane and decreasing the proton motive force. This ultimately leads to the disruption of the membrane potential. However, the exact mechanism behind this phenomenon has not been fully described (28). Several metal ions exhibit wide ranging antimicrobial spectrum, targeting various cellular components. The range of activities exhibited by this spectrum is typically attributed to the unique features of the metal, which enable its interactions with pertinent functional groups in biological molecules. The selectivity and specificity of metal binding, which is closely linked to its

antimicrobial efficacy (31). The process of choosing metals for their interaction with various active groups in metabolites. Proteins, nucleic acids, lipids and carbohydrates is contingent upon the specific properties of the metal. This choice is made due to the potential for any of these cellular components to initiate harmful cascading reactions. The impact of the preceding cascade can be categorized into several distinct areas. The various mechanisms of cellular damage encompass direct and indirect effects on the cell membrane, such as impairment of its integrity, changes in membrane potential and transport processes as well as protein dysfunction leading to metabolic disturbances and denaturation. Additionally, cellular damage can manifest through the impairment of the electron transport chain, DNA damage and conformational changes, inhibition of DNA replication and repair mechanisms and degradation of carbohydrates (32).

Conclusion

It is obvious that the industry of making juice from *Citrus sinensis* generates enormous quantity of wastes, like as peel, seeds and pomace. Therefore, improper management of these wastes will harm the environment and result in a loss of this treasure. Various food and pharmaceutical businesses can successfully use orange byproducts as flavoring ingredients, sources of fiber and pectin, or as antifungal and antibacterial agents. Green synthesis gold nanoparticles from synephrine and uses it as anti-fungal, the activity of nanoparticles more than candstatin that uses in treatment of dermatophyte.

Acknowledgements

This research was fully funded by the Ministry of Higher Education, Malaysia

Compliance with ethical standards

Conflict of interest: Author declared there was no conflict of interest.

Ethical issues: None.

References

1. Segal E, Elad D. Human and zoonotic dermatophytoses: Epidemiological aspects. *Frontiers in Microbiology*. 2021;12. <https://doi.org/10.3389/fmicb.2021.713532>

2. Hossain CM, Ryan LK, Gera M, Choudhuri S, Lyle N, Ali KA *et al.* Antifungals and drug resistance. *Encyclopedia*. 2022;2(4):1722-37. <https://doi.org/10.3390/encyclopedia2040118>
3. Chanyachailert P, Leeyaphan C, Bunyaratavej S. Cutaneous fungal infections caused by dermatophytes and non-dermatophytes: An updated comprehensive review of epidemiology, clinical presentations and diagnostic testing. *Journal of Fungi*. 2023;9(6):669. <https://doi.org/10.3390/jof9060669>
4. Stohs SJ, Shara M, Ray SD. p-synephrine, ephedrine, p-octopamine and m-synephrine: Comparative mechanistic, physiological and pharmacological properties. *Phytotherapy Research*. 2020;34(8):1838-46. <https://doi.org/10.1002/ptr.6649>
5. Zhang Y, You Z, Liu L, Duan S, Xiao A. Electrochemical determination of synephrine by using nafion/UiO-66/graphene-modified screen-printed carbon electrode. *Current Research in Food Science*. 2022;5:1158-66. <https://doi.org/10.1016/j.crf.2022.07.008>
6. Ruiz-Moreno C, Del Coso J, Giráldez-Costas V, González-García J, Gutiérrez-Hellín J. Effects of p-synephrine during exercise: A brief narrative review. *Nutrients*. 2021;13(1):233. <https://doi.org/10.3390/nu13010233>
7. Khan I, Saeed K, Khan I. Nanoparticles: Properties, applications and toxicities. *Arabian Journal of Chemistry*. 2019;12(7):908-31. <https://doi.org/10.1016/j.arabj.2017.05.011>
8. Svendsen C, Walker LA, Matzke M, Lahive E, Harrison S, Crossley A *et al.* Key principles and operational practices for improved nanotechnology environmental exposure assessment. *Nature Nanotechnology*. 2020;15(9):731-42. <https://doi.org/10.1038/s41565-020-0742-1>
9. Rabha B, Bharadwaj KK, Boro N, Ghosh A, Gogoi SK, Varma RS *et al.* *Cheilocostus speciosus* extract-assisted naringenin-encapsulated poly-ε-caprolactone nanoparticles: Evaluation of anti-proliferative activities. *Green Chemistry*. 2021;23(19):7701-11. <https://doi.org/10.1039/D1GC02260A>
10. Andleeb A, Andleeb A, Asghar S, Zaman G, Tariq M, Mehmood A *et al.* A systematic review of biosynthesized metallic nanoparticles as a promising anti-cancer-strategy. *Cancers*. 2021;13(11):2818. <https://doi.org/10.3390/cancers13112818>
11. Jasim AR, Hussein A, Nasser A. Phytochemical investigation of synephrine in the fruit peels of Iraqi sour orange. *World J Pharm Pharm Sci*. 2016;5:246.
12. Muneeswari VS, Karthick S, Akanksha D, Sushma G, Hasheem SA, Vasimunni S *et al.* Extraction and identification of phytochemical active constituents in leaves of *Catharanthus roseus*, *Carica papaya* and *Piper betel* by using TLC method. *World Journal of Pharmaceutical Research*. 2022;11(10):891-937.
13. Sun Y, Xia X, Yuan G, Zhang T, Deng B, Feng X *et al.* Stachydrine, a bioactive equilibrist for synephrine, identified from four citrus chinese herbs. *Molecules*. 2023;28(9):3813. <https://doi.org/10.3390/molecules28093813>
14. Yadav B, Singla A, Srivastava N, Gupta P. Pharmacognostic and phytochemical screening of *Datura stramonium* by TLC and GC-MS: A forensic approach. *Biomedical and Pharmacology Journal*. 2021;14(4):2221-26. <https://doi.org/10.13005/bpj/2320>
15. Ahmed S, Saifullah, Ahmad M, Swami BL, Ikram S. Green synthesis of silver nanoparticles using *Azadirachta indica* aqueous leaf extract. *Journal of Radiation Research and Applied Sciences*. 2016;9(1):1-7. <https://doi.org/10.1016/j.jrras.2015.06.006>
16. Barnawi N, Allehyani S, Seoudi R. Biosynthesis and characterization of gold nanoparticles and its application in eliminating nickel from water. *Journal of Materials Research and Technology*. 2022;17:537-45. <https://doi.org/10.1016/j.jmrt.2021.12.013>
17. Mayeen A, Shaji LK, Nair AK, Kalarikkal N. Chapter 12 - Morphological characterization of nanomaterials. In: Mohan Bhagyaraj S, Oluwafemi OS, Kalarikkal N, Thomas S editors. *Characterization of Nanomaterials*: Woodhead Publishing. 2018;p.335-64. <https://doi.org/10.1016/B978-0-08-101973-3.00012-2>
18. Rautela A, Rani J, Debnath M. Green synthesis of silver nanoparticles from *Tectona grandis* seeds extract: Characterization and mechanism of antimicrobial action on different microorganisms. *Journal of Analytical Science and Technology*. 2019;10(1):5. <https://doi.org/10.1186/s40543-018-0163-z>
19. Wens A, Geuens J. *In vitro* and *in vivo* antifungal activity of plant extracts against common phytopathogenic fungi. *Journal of BioScience and Biotechnology*. 2022;11(1):15-21.
20. Jayaseelan C, Rahuman AA, Kirthi AV, Marimuthu S, Santhoshkumar T, Bagavan A *et al.* Novel microbial route to synthesize ZnO nanoparticles using *Aeromonas hydrophila* and their activity against pathogenic bacteria and fungi. *Spectrochimica Acta Part A: Molecular and Biomolecular Spectroscopy*. 2012;90:78-84. <https://doi.org/10.1016/j.saa.2012.01.006>
21. Park J, Lim D-H, Lim H-J, Kwon T, Choi J-s, Jeong S *et al.* Size dependent macrophage responses and toxicological effects of Ag nanoparticles. *Chemical Communications*. 2011;47(15):4382-84. <https://doi.org/10.1039/c1cc10357a>
22. Eid MM. Characterization of nanoparticles by FTIR and FTIR-microscopy. *Handbook of Consumer Nanoproducts*. Singapore: Springer Singapore. 2021;p.1-30. https://doi.org/10.1007/978-981-15-6453-6_89-1
23. McKeny P, Nessel T, Zito P. Antifungal antibiotics. [Updated 2021 Nov 15]. *StatPearls* [Internet] Treasure Island (FL): StatPearls Publishing. 2022.
24. Al-Zubaidi AM, Abd MM, Al-Bahrani RM. The antagonistic effect of biosynthesized nanoparticles from aqueous extract of *Agaricus bisporus* on some pathogenic plant fungi. *HIV Nursing*. 2022;22(2):113-15.
25. Jalal H, Buchanich JM, Roberts MS, Balmert LC, Zhang K, Burke DS. Changing dynamics of the drug overdose epidemic in the United States from 1979 through 2016. *Science*. 2018;361(6408):eaau1184. <https://doi.org/10.1126/science.aau1184>
26. Jadou A, Al-Shahwany AW. Biogenic synthesis and characterization of silver nanoparticles using some medical plants and evaluation of their antibacterial and toxicity potential. *Journal of AOAC International*. 2019;101(6):1905-12. <https://doi.org/10.5740/jaoacint.17-0500>
27. Bribi N. Pharmacological activity of alkaloids: A review. *Asian Journal of Botany*. 2018;1(1):1-6.
28. Joseph J, Keren DS, Raghavi R, Mary SA, Aruni W. Green synthesis of silver nanoparticles using *Phyllanthus amarus* seeds and their antibacterial activity assessment. *Biomedical and Biotechnology Research Journal (BBRJ)*. 2021;5(1):35-38. https://doi.org/10.4103/bbrj.bbrj_139_20
29. Yass M, Al-Haddad A, Ali MJM, Jaafar A, Veres M. Effectiveness of green synthesized zinc oxide nanoparticles against extensively drug-resistant *Klebsiella pneumoniae*. *Biomedical and Biotechnology Research Journal (BBRJ)*. 2023;7(3):497-503.
30. Kubacka A, Diez MS, Rojo D, Bargiela R, Ciordia S, Zapico I *et al.* Understanding the antimicrobial mechanism of TiO₂-based nanocomposite films in a pathogenic bacterium. *Scientific Reports*. 2014;4(1):4134. <https://doi.org/10.1038/srep04134>
31. Widadalla HA, Yassin LF, Alrasheid AA, Ahmed SAR, Widadallah MO, Eltilib SH *et al.* Green synthesis of silver nanoparticles using green tea leaf extract, characterization and evaluation of antimicrobial activity. *Nanoscale Advances*. 2022;4(3):911-15. <https://doi.org/10.1039/D1NA00509J>
32. Kadiyala U, Turali-Emre ES, Bahng JH, Kotov NA, VanEpps JS. Unexpected insights into antibacterial activity of zinc oxide nanoparticles against methicillin resistant *Staphylococcus aureus* (MRSA). *Nanoscale*. 2018;10(10):4927-39. <https://doi.org/10.1039/C7NR08499D>